Journal of Dental Sciences (2018) 13, 354–359

Available online at www.sciencedirect.com

ScienceDirect

journal homepage: www.e-jds.com

Original Article

Dynamic imaging of the effect of mesenchymal stem cells on osteoclast precursor cell chemotaxis for bone defects in the mouse skull

Takaharu Abe [a], Keisuke Sumi [a], Ryo Kunimatsu [a*], Nanae Oki [a], Yuji Tsuka [a], Kengo Nakajima [a], Kotaro Tanimoto [b]

[a] *Department of Orthodontics, Division of Oral Health and Development, Hiroshima University Hospital, Japan*
[b] *Department of Orthodontics and Craniofacial Developmental Biology, Hiroshima University Graduate School of Biomedical & Health Sciences, Japan*

Received 5 June 2018; Final revision received 20 July 2018
Available online 24 August 2018

KEYWORDS
Bone regeneration;
Chemotaxis;
Mesenchymal stem cells;
RAW264 cells

Abstract *Background/purpose:* Mesenchymal stem cells (MSCs) transplantation has previously been used in the field of regenerative medicine. Although bone regeneration is known to occur through the interaction between osteoblasts and osteoclasts, the effect of MSCs on osteoclasts is unknown. Therefore, the purpose of this study was to investigate the effect of MSCs on the chemotaxis of osteoclast precursor cells (RAW264 macrophage cells).
Materials and methods: Bone defects were created in mice skulls, and MSCs and a scaffold of carbonated hydroxyapatite were transplanted into the bone defects. RAW264 cells were then transplanted into the mouse tail vein, and their dynamics were observed by an *in vivo* imaging system.
Results: The fluorescent intensity of the MSCs transplant group at the bone defect region was significantly higher on days 3, 5, and 7 compared with the MSCs non-transplant group.
Conclusion: Increased RAW264 chemotaxis to the bone defect region occurred following the simultaneous implantation of MSCs in the skull defect.

* Corresponding author. Department of Orthodontics, Division of Oral Health and Development, Hiroshima University Hospital, 1-2-3 Kasumi, Minami-ku, Hiroshima 734-8553, Japan. Fax: +81 82 257 5687.
E-mail address: ryoukunimatu@hiroshima-u.ac.jp (R. Kunimatsu).

https://doi.org/10.1016/j.jds.2018.08.001

Introduction

The evaluation of cell transplantation experiments has mainly been conducted by histological examination. However, it is not possible to evaluate the same laboratory animal when assessing experiments over time. Therefore, *in vivo* imaging is a useful method to evaluate cellular dynamics within the body.[1]

Mesenchymal stem cells (MSCs) are relatively easy to harvest and cultivate, and have bone differentiation capabilities, so are often used for bone regeneration experiments. The paracrine effect of growth factors, cytokines, and chemokines secreted by MSCs is believed to promote bone repair and to affect the dynamics of other cells.[2–4] Therefore, cell chemotactic factors are being recognized as useful elements for bone regeneration.

Osugi et al.[5] previously reported the enhancement of MSCs chemotaxis using an *in vivo* imaging system. However, although macrophages have been shown to accumulate at MSCs,[6] few reports have been conducted over time using *in vivo* imaging. We have carried out bone regeneration treatment involving the transplantation of MSCs and carbonated hydroxyapatite (CAP) scaffolds to artificial bone defects in the jaw cleft of beagle dogs.[7] Furthermore, it has been revealed that MSCs promote cell chemotaxis *in vitro* by the RAW264 macrophage paracrine factor.[8] However, the *in vivo* details of these mechanisms remain unclear. In the present study, we used an *in vivo* imaging device to investigate the dynamics of MSCs after transplantation and the chemotaxis-promoting effect on RAW264 cells involving the paracrine mechanism.

Materials and methods

Cell culture

We used Balb/c mouse bone marrow-derived MSCs (Cyagen Biosciences, Santa Clara, CA, USA). The cells were cultured according to the supplier's recommendations and as previously reported,[9] and were used for experiments during passages 8—11. The Balb/c mouse cell line RAW264, as an osteoclast precursor (Riken Cell Bank no. RCB 0535, RIKEN, Tokyo, Japan), was cultured as recommended by the suppliers and as previously reported.[10] Cells were used for experiments during passages 6—9. MSCs and RAW264 cells were cultured in α-minimum essential medium (α-MEM; Sigma Aldrich, St. Louis, MO, USA) supplemented with 10% fetal bovine serum (Biological Industries, Hartford, CS, USA), 10% sodium bicarbonate, and 0.7 mg/ml L-glutamine. All cultures were incubated at 37 °C in a humidified atmosphere with 5% CO_2.

Experimental animals and feed

Male Balb/c nude mice (Japan Charles River, Yokohama, Japan) at 6 weeks of age were used as experimental animals. D10001 solid food (AIN-76A; Research Diet, EPS Masuzo, Tokyo, Japan) without a fluorescent component (alfalfa-free feed) was provided, from 1 week before the start of experiment. Animal experiments were approved by the Animal Experiment Committee of Hiroshima University (A15-137).

MSC transplantation and time course of localization and survival

Prior to the experiment, CAP was polished to a diameter of 4 mm and a thickness of 0.5 mm using a Grinder Polisher Model 900 (South Bay Technology, San Clemente, CA, USA), and gas sterilization was performed.

Three mice were anesthetized using 10% somnopentyl (Kyoritsu Pharmaceutical, Tokyo, Japan) and 10% atropine sulfate (Wako, Tokyo, Japan). Subsequently, skin incisions were made at the top of the head, and the periosteum was detached. Then, bone defects 5 mm in diameter were made using a dental low-speed engine (Nagata Electric Co., Tokyo, Japan) and a 5-mm diameter trephine bur (Implatex, Tokyo, Japan). CAP was then implanted into the defect site, and the skin was tightly sutured.

After 5 days, the wound site was closed. MSCs were then labeled with the cellular fluorescent labeling reagent DiD (Thermo Fisher Science, Carlsbad, CA, USA), which has an excitation wavelength of 644 nm and a fluorescence wavelength of 665 nm, and were suspended in α-MEM at 1.0×10^6 cells/ml. A Flowmax 30 G × 1/2 RB GA needle (NIPRO, Osaka, Japan) was then attached to a 1.0 ml Terumo syringe (Terumo, Tokyo, Japan), and 100 μl MSCs (1.0×10^5 cells) were transplanted into the subcutaneous skull defect area of three mice. The region was observed using the IVIS Spectrum CT system (Sumisho Pharma International, Tokyo, Japan) just before transplantation, 1 day after transplantation, and daily thereafter. Isoflurane inhalation anesthesia (Mylan, Canonsburg, PA, USA) was used during observation of the mice. The fluorescence intensity was measured by designating a circular region (2.965 cm^2) covering the bone defect site with the region of interest tool. The state before MSCs transplantation was known as "pre". Measurements were carried out every 2 days from day 1.

Accumulation of RAW264 cells in mouse skull defects

CAP was implanted into mouse bone defect sites and the skin was sutured as described above. After 5 days, the wound site was closed. In the experimental group (MSCs (+)), 100 μl unlabeled MSCs (1×10^5 cells) were transplanted into the subcutaneous skull defect area. After that, RAW264 cells fluorescently labeled with DiD (Thermo Fisher Science) were resuspended at 4.0×10^6 cells/ml, then 500 μl (2.0×10^6 cells) was injected with 20 U/ml heparin into the mouse tail vein. In the non-transplant group (MSCs (−)), 100 μl α-MEM was injected into the skull defect area, then fluorescently labeled RAW264 cells (500 μl, 2.0×10^6 cells) with 20 U/ml heparin were transplanted into the tail vein. In the control group, no skull defect was created, 100 μl α-MEM was transplanted into skull area and RAW264 cells (500 μl, 2.0×10^6 cells) with 20 U/ml heparin were transplanted into the tail vein. Each of the three groups contained six mice, an comparisons were made among the three groups. The state before RAW264 cell transplantation was known as "pre". Measurements were made every 2 days from day 1.

Statistical analysis

Results are expressed as the mean ± SD. Multiple comparisons were analyzed using the Bonferroni/Dunn method. Significance was defined as $p < 0.05$ and 0.01.

Results

Time course of MSC localization

After the transplant, fluorescently-labeled MSCs were shown to accumulate around the bone defect region (Fig. 1A). The fluorescence intensity decreased over time, and by 15 days after transplantation had decreased to about 30% of the level detected 1 day after transplantation (Fig. 1B).

RAW264 cell accumulation

After transplanting MSCs and CAP to the mouse skull defect, RAW264 cells were injected into the tail vein and found to accumulate at the transplant area. In the control group, RAW264 accumulation was observed at the kidney and the spine, but the fluorescence intensity was low and no significant accumulation was seen at the skull defect region (Fig. 2A). In the MSC non-transplant group, RAW264 accumulation at the bone defect region and the middle of the spine occurred 1 day after transplantation. In the MSC transplant group, extensive RAW264 accumulation was observed from the bone defect region to the upper part of the spine, as well as around the skull defect region.

The fluorescence intensity of the MSCs transplant group at the bone defect part was significantly higher on days 3, 5, and 7 ($p < 0.01$) and on days 1 and 9 ($p < 0.05$) compared with the control group (Fig. 2B), and significantly higher on days 3, 5, and 7 compared with the MSCs non-transplant group ($p < 0.05$).

Discussion

The dynamics of immune cells such as macrophages and neutrophils have been extensively studied using molecular

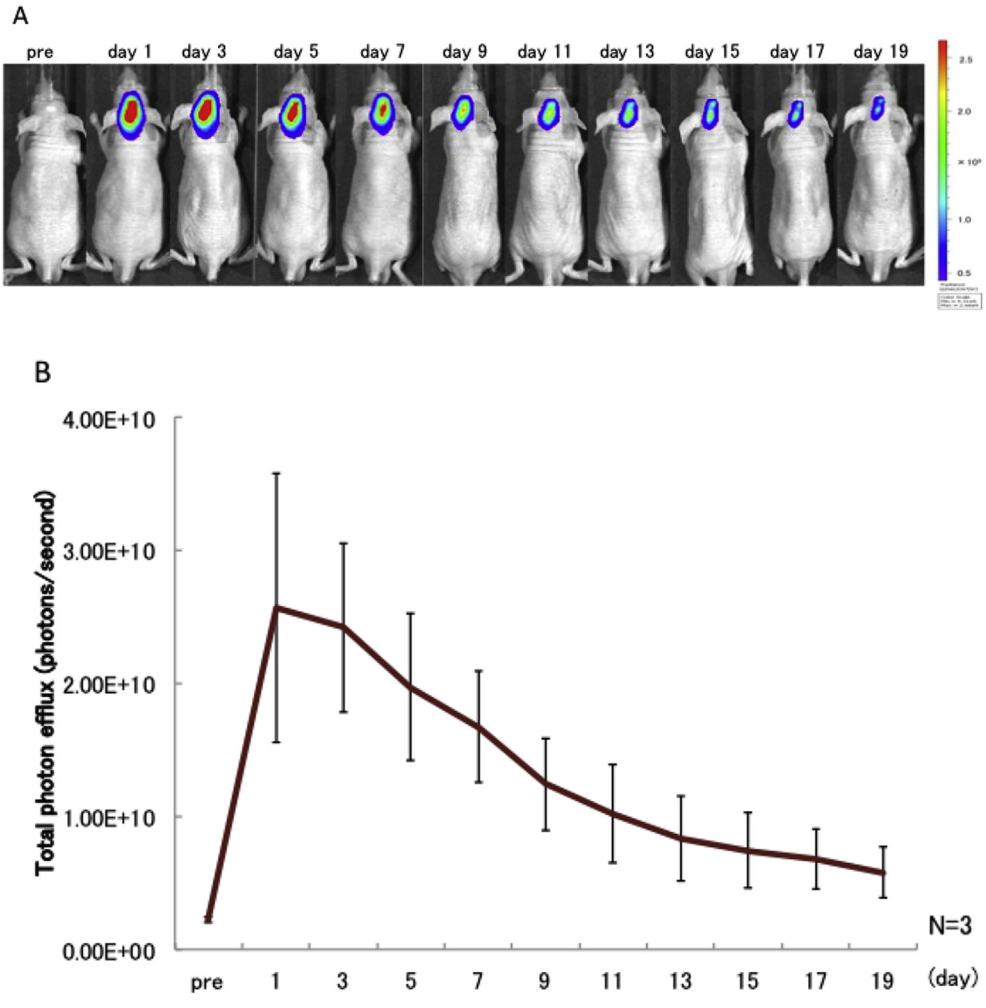

Figure 1 A bone defect was created in the mouse cranium, and MSCs fluorescently labeled with Did were implanted into the cranium on day 5. Fluorescence observation was carried out after cranial skin healing. (A) Imaging of the dynamics of transplant MSCs. "pre": the state before MSC transplantation. Fluorescence was measured every 2 days from day 1. (B) Fluorescence intensity in the cranium of mice receiving transplanted MSCs. Values represent means ± SD ($n = 3$).

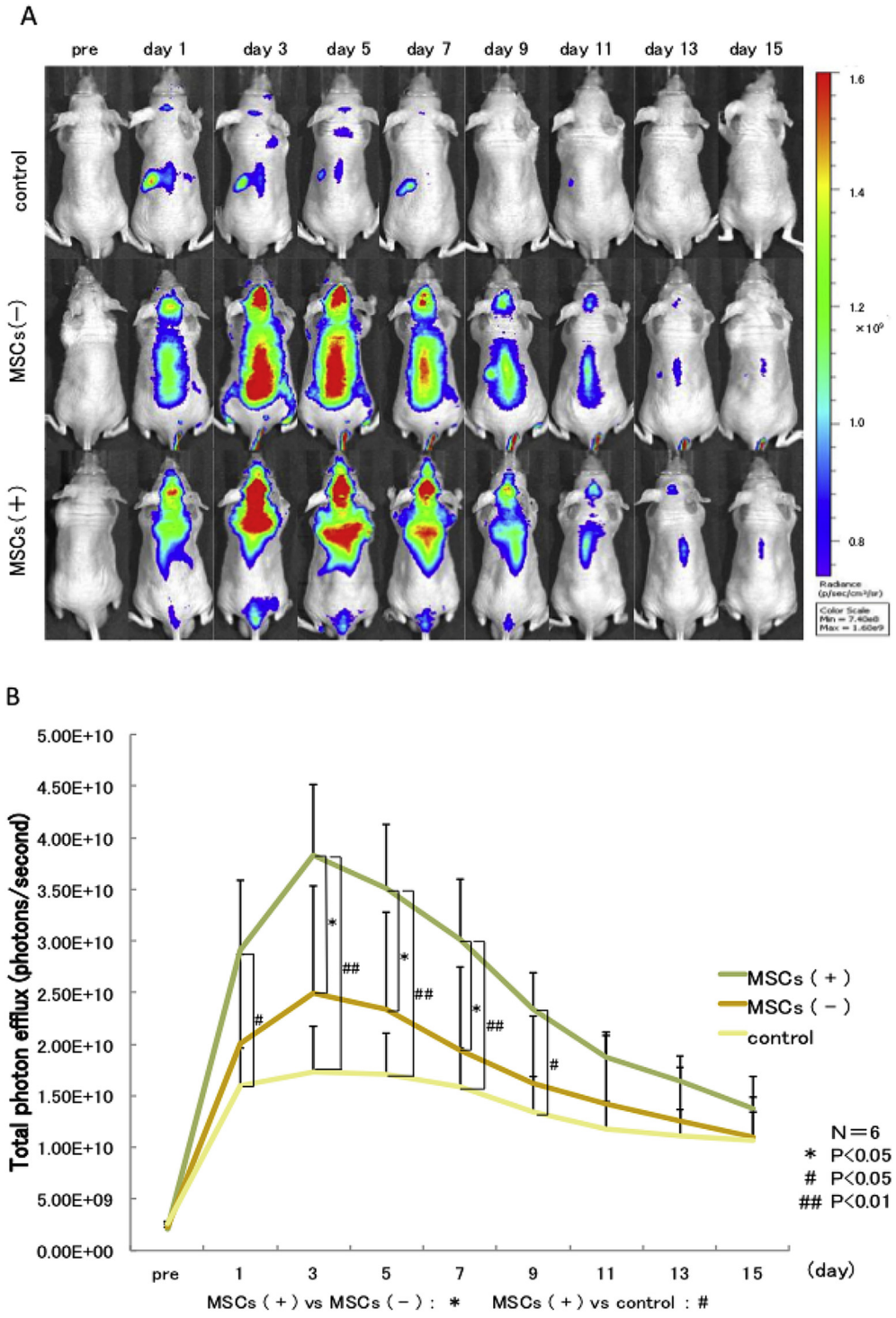

Figure 2 A bone defect was created in the cranium. After 5 days, unlabeled MSCs were transplanted into the defect area, and RAW264 cells fluorescently labeled with Did were transplanted into the tail vein. (A) Imaging of the dynamics of transplanted RAW264 cells. MSCs (+): MSCs were transplanted into the skull defect area, and RAW264 cells were transplanted into the tail vein; MSCs (−): α-MEM was delivered to the skull defect area, and RAW264 cells were transplanted into the tail vein; control: no skull defect was created, α-MEM was delivered to the skull defect area, and RAW264 cells were transplanted into the tail vein. (B) Fluorescence intensity of RAW264 cells at the cranial region. Only one side of the 1 SD error bar is shown. Values represent means ± SD (n = 6).

imaging technique,[7,11,12] of which cell tracking using *in vivo* imaging is particularly useful. In this study, transplanted MSCs were shown to remain around the transplant region for more than 19 days. This is consistent with the findings by Kidd et al.,[13] and suggested that MSCs accumulate around sites of damage and repair.

We also observed that 15 days after transplantation, the fluorescence intensity had decreased to ~30% compared with 1 day after transplantation. This could reflect dilution of the pigment through cell differentiation and proliferation, cell diffusion, or cell death. Indeed, Gamblin et al.[14] reported a decrease in fluorescence by 15% between 2 and 4 weeks after MSCs transplantation, and Kinnaird et al.[2] documented its disappearance after 2—3 weeks. Becquart et al.[15] previously attributed a reduction in MSC number to ischemia, and Deschepper et al.[16] reported it to be caused by a reduction in glucose levels.

In our preliminary *in vitro* experiments, we confirmed that sufficient fluorescence intensity of MSCs could be maintained for around 3 weeks. Therefore, our observed *in vivo* decrease in fluorescence intensity most likely reflects a reduction in cell number. It is also possible that cell division caused the decrease in fluorescence intensity; this could be overcome in the future by the introduction of luciferase, which is not affected by cell proliferation. However, it is relatively difficult to transduce genes into RAW264 cells,[17] so this could prove technically challenging.

The fluorescence intensity of the transplant area was significantly higher in the MSC transplant group than in the MSC non-transplant group. This is probably because RAW264 cells accumulated at the skull defect area through the chemotactic action of MSCs. By comparison, there was no significant difference in fluorescence intensity between the MSC non-transplant group and the control group, although accumulation at the skull defect area and the middle of the spine was observed. Accumulation at the bone defect area may have occurred through an increase in blood flow and the influence of chemokines during inflammation, while accumulation at the dorsal region could reflect the inherent fluorescence of RAW264 cells circulating around the spinal artery and veins.

In the MSC transplant group, accumulation of RAW264 cells was observed above the dorsal region, which may correspond to brown adipose tissue as reported by Zhang et al.[18] Because macrophage activities and chemotaxis are enhanced by adipocyte-derived factors,[19] this suggests that MSCs activate brown fat and accumulate above the dorsum. Macrophages are known to accumulate during early-stage inflammation,[20] and we observed increased RAW264 cell accumulation following the transplantation of MSCs in the present study. This was consistent with the findings of Gamblin et al.[14] Macrophages have been reported to differentiate into osteoclasts through the influence of RANKL expressed by osteoblasts and osteocytes.[21] At first glance, from the results of this study, macrophages seem to promote bone resorption. However, osteoclasts promote osteogenesis through resorption activity,[22] and are necessary for normal bone remodeling.[23] Furthermore, the chemotaxis of MSCs and other remodeling cells was shown to be enhanced by MSCs,[5,24] suggesting that they improve the bone remodeling function. Further discussion of this function is required.

In conclusion, we observed the *in vivo* accumulation of RAW264 cells following MSCs transplants to mouse skull bone defects, and inferred that they were involved in bone remodeling. Dramatic advances in imaging technology have enabled intracellular organelle sorting and fluorescent protein vectors to be examined *in vitro*, and internal bone structures to be observed using two-photon excitation microscopes.[25,26] These techniques should allow more detailed cell dynamics to be elucidated in the future, which is of importance in achieving a high therapeutic effect in the affected area.

Conflicts of interest

The authors have no conflicts of interest to declare.

Acknowledgments

This work was carried out at the Research Center for Molecular Medicine, Hiroshima University. This work was funded by a grant from the JSPS KAKENHI (No. 15K20595). We thank Sarah Williams, PhD, from Edanz Group (www.edanzediting.com) for editing a draft of this manuscript.

References

1. Contag CH, Jenkins D, Contag PR, Negrin RS. Use of reporter genes for optical measurements of neoplastic disease in vivo. *Neoplasia* 2000;21:41—52.
2. Kinnaird T, Stabile E, Burnett MS, et al. Local delivery of marrow-derived stromal cells augments collateral perfusion through paracrine mechanisms. *Circulation* 2004;109:1543—9.
3. Ponte AL, Marais E, Gallay N, et al. The in vitro migration capacity of human bone marrow mesenchymal stem cells: comparison of chemokine and growth factor chemotactic activities. *Stem Cell* 2007;25:1737—45.
4. Schenk S, Mal N, Finan A, et al. Monocyte chemotactic protein-3 is a myocardial mesenchymal stem cell homing factor. *Stem Cell* 2007;25:245—51.
5. Osugi M, Katagiri W, Yoshimi R, Inukai T, Hibi H, Ueda M. Conditioned media from mesenchymal stem cells enhanced bone regeneration in rat calvarial bone defects. *Tissue Eng Pt A* 2012;18:1479—89.
6. Ren G, Zhao X, Wang Y, et al. CCR2-dependent recruitment of macrophages by tumor-educated mesenchymal stromal cells promotes tumor development and is mimicked by TNFα. *Cell Stem Cell* 2012;11:812—24.
7. Yoshioka M, Tanimoto K, Tanne Y, et al. Bone regeneration in artificial jaw cleft by use of carbonated hydroxyapatite particles and mesenchymal stem cells derived from Iliac Bone. *Int J Dent* 2012;2012:1—8.
8. Sumi K, Abe T, Kunimatsu R, et al. The effect of mesenchymal stem cells on chemotaxis of osteoclast precursor cells. *J Oral Sci* 2018;60:221—5.
9. Liu RH, Li YQ, Zhou WJ, Shi YJ, Ni L, Liu GX. Supplementing mesenchymal stem cells improves the therapeutic effect of hematopoietic stem cell transplantation in the treatment of murine systemic lupus erythematosus. *Transplant Proc* 2014;46:1621—7.
10. Suzuki N, Yoshimura Y, Deyama Y, Suzuki K, Kitagawa Y. Mechanical stress directly suppresses osteoclast differentiation in RAW264.7 cells. *Int J Mol Med* 2008;21:291—6.

11. Ren PG, Lee SW, Biswal S, Goodman SB. Systemic trafficking of macrophages induced by bone cement particles in nude mice. *Biomaterials* 2008;29:4760—5.
12. Seo JH, Jeon YH, Lee YJ, et al. Trafficking macrophage migration using reporter gene imaging with human sodium iodide symporter in animal models of inflammation. *J Nucl Med* 2010;51:1637—43.
13. Kidd S, Spaeth E, Dembinski JL, et al. Direct evidence of mesenchymal stem cell tropism for tumor and wounding microenvironments using in vivo bioluminescent imaging. *Stem Cell* 2009;27:2614—23.
14. Gamblin AL, Brennan MA, Renaud A, et al. Bone tissue formation with human mesenchymal stem cells and biphasic calcium phosphate ceramics: the local implication of osteoclasts and macrophages. *Biomaterials* 2014;35:9660—7.
15. Becquart P, Cambon-Binder A, Monfoulet LE, et al. Ischemia is the prime but not the only cause of human multipotent stromal cell death in tissue-engineered constructs in vivo. *Tissue Eng Pt A* 2012;18:2084—94.
16. Deschepper M, Manassero M, Oudina K, et al. Proangiogenic and prosurvival functions of glucose in human mesenchymal stem cells upon transplantation. *Stem Cell* 2013;31:526—35.
17. Cheung ST, Shakibakho S, So EY, Mui A. Transfecting RAW264.7 cells with a luciferase reporter gene. *J Vis Exp* 2015;2015, e52807.
18. Zhang X, Kuo C, Moore A, Ran C. In vivo optical imaging of interscapular brown adipose tissue with 18F-FDG via cerenkov luminescence imaging. *PLoS One* 2013;8:1—10.
19. Xu H, Barnes G, Yang Q, et al. Chronic inflammation in fat plays a crucial role in the development of obesity-related insulin resistance. *J Clin Invest* 2003;112:1821—30.
20. Ono T, Takayanagi H. Osteoimmunology in bone fracture healing. *Curr Osteoporos Rep* 2017;15:367—75.
21. Honma M, Ikebuchi Y, Kariya Y, et al. RANKL subcellular trafficking and regulatory mechanisms in osteocytes. *J Bone Miner Res* 2013;28:1936—49.
22. Pasuri J, Holopainen J, Kokkonen H, et al. Osteoclasts in the interface with electrospun hydroxyapatite. *Colloids Surf B Biointerfaces* 2015;135:774—83.
23. Walker EC1, McGregor NE, Poulton IJ, et al. Cardiotrophin-1 is an osteoclast-derived stimulus of bone formation required for normal bone remodeling. *J Bone Miner Res* 2008;23:2025—32.
24. Ando Y, Matsubara K, Ishikawa J, et al. Stem cell-conditioned medium accelerates distraction osteogenesis through multiple regenerative mechanisms. *Bone* 2014;61:82—90.
25. Gupta R, Srivastava OP. Identification of interaction sites between human betaA3 — and alphaA/alphaB-crystallins by mammalian two-hybrid and fluorescence resonance energy transfer acceptor photobleaching methods. *J Bio Chem* 2009; 284:18481—92.
26. Wake H, Moorhouse AJ, Jinno S, Kohsaka S, Nabekura J. Resting microglia directly monitor the functional state of synapses in vivo and determine the fate of ischemic terminals. *J Neurosci* 2009;29:3974—80.